Available online at www.sciencedirect.com
ScienceDirect
Ceramics International 36 (2010) 2365–2374
CERAMICS INTERNATIONAL
www.elsevier.com/locate/ceramint

A study on the interfacial reaction and dielectric properties of $Ba_{0.88}(Nd_{1.40}Bi_{0.42}La_{0.30})Ti_4O_{12}$/alkali-borosilicate glass composites

Kuan-Hong Lin [a,*], Chang-Lun Liao [b], Shun-Tian Lin [b]

[a] Department of Mechanical Engineering, Tungnan University, Taipei 222, Taiwan, ROC
[b] Department of Mechanical Engineering, National Taiwan University of Science and Technology, Taipei 106, Taiwan, ROC

Received 11 March 2010; received in revised form 3 April 2010; accepted 14 June 2010
Available online 3 August 2010

Abstract

This study investigated the effects of sintering parameters and the addition of alkali-borosilicate glass into the $Ba_{0.88}(Nd_{1.40}Bi_{0.42}La_{0.30})Ti_4O_{12}$ B(NBL)T ceramic. The microstructure evolution, ionic exchange phenomenon at phase interfaces and the dielectric properties variation of composites were examined by XRD, EPMA, TEM, RF impedance analyzer and network analyzer, respectively. XRD patterns revealed that interactions between B(NBL)T ceramic and glass during sintering could have caused the change in the preferred orientation as well as the shifting of the crystals' diffraction angles. EPMA mapping showed that the concentrations of Ba, and Bi decreased along the edge of the B(NBL)T ceramic that is closest to the glass phase, while the opposite trend was seen for Na and Ca. TEM and EDS analyses confirm that an ionic exchange took place during sintering with the glass phase wetting the B(NBL)T ceramic and was responsible for the change in the crystal plane and the variation in lattice parameters. The ionic exchange that occurred between the B(NBL)T ceramic and the glass phase resulted in a decrease in the electrical resistivity of the glass phase, which in turn reduced the dielectric loss.

Keywords: A. Sintering; B. Composites; B. Microstructure-final; C. Dielectric properties

1. Introduction

Most well-known commercial microwave dielectric materials exhibit a high dielectric constant (ε_r), a high quality factor (Q), and very low temperature coefficients of the resonant frequency (τ_f) [1–4]. For these classical microwave dielectric materials to reach superior dielectric properties, a very high sintering temperature, ranging from about 1200 °C to 1400 °C, is required [5,6]. However, if these dielectric materials are to be co-fired with silver conductors, the sintering temperature of the dielectric materials must be lower than the melting point of silver (961 °C). The most common approach to reducing the sintering temperature of a microwave dielectric ceramic is to add sintering aids or glass with low melting temperatures [2,6,7]. For example, $BaO(Nd_{0.8}Bi_{0.2})_2O_34TiO_2$ added with 10 wt.% Li_2O–B_2O_3–SiO_2–Al_2O_3–CaO glass could be sintered at 900 °C, yielding a composite structure having a quality factor ($Q \times f$) of 2200 GHz, an ε_r of 68, and a τ_f of 55 ppm/°C [5]. Similar trends were observed in the $BaNd_2Ti_4O_{12}$ microwave ceramic, in which B_2O_3–Bi_2O_3–SiO_2–ZnO or La_2O_3–B_2O_3–TiO_2 glass was added to reduce the sintering temperature [8,9]. It was also shown that alumina and silica based glasses were more effective in improving the dielectric properties of $Ca_5Nb_2TiO_{12}$ ceramics, whereas borate glasses are preferred for lowering the sintering temperature.

On the other hand, although a glass phase additive could reduce the sintering temperature, it was shown that a larger amount of glass added to $Ca_5Nb_2TiO_{12}$ caused increased porosity, resulting in reduced dielectric properties [10]. Researchers have also reported that $La_4Ti_9O_{24}$ ceramics added with 20 vol.% PbO–B_2O_3–SiO_2 and ZnO–B_2O_3–SiO_2 glass could be sintered at 1000 °C, yielding a composite structure having a 95% theoretical density. The interaction between PbO–B_2O_3–SiO_2 and $La_4Ti_9O_{24}$ results in the formation of a secondary phase $La_{2/3}TiO_3$, which strongly influences the dielectric properties of $La_4Ti_9O_{24}$ ceramics [11]. Jung et al. [9] indicated that the $BaNd_2Ti_4O_{12}$ (BNT) ceramic added with La_2O_3–B_2O_3–TiO_2 (LBT) glass could be sintered at 850 °C,

* Corresponding author. Tel.: +886 2 86625917; fax: +886 2 86625919.
E-mail address: khlin@mail.tnu.edu.tw (K.-H. Lin).

0272-8842/$36.00
doi:10.1016/j.ceramint.2010.07.021

yielding a dielectric constant of 20, a quality factor ($Q \times f$) of 8000 GHz, and a low temperature coefficient of resonant frequency ($\tau_f = 76.8$ ppm/°C) at frequencies ranging from 6 GHz to 7 GHz. The most significant sintering result was the formation of HT-$LaBO_3$ (high temperature forming) and TiO_2 due to the reaction between the BNT ceramic and LBT glass. The reaction products played positively in improving the microwave dielectric properties of BNT ceramics. Lee et al. [12] added B_2O_3 to $BaTi_4O_9$ ceramics and observed active dissolution of Ba and Ti atoms from $BaTi_4O_9$ into B_2O_3 liquid, leading to the formation of many secondary phases, such as $Ba_2Ti_9O_{20}$, $BaTi(BO_3)_2$, TiO_2, and, many large pores were formed by B_2O_3. These results deteriorated the dielectric characteristics of $BaTi_4O_9$. Chang et al. [13] added Al_2O_3-doped silica glass to the BaO–Nd_2O_3–Sm_2O_3–TiO_2 microwave materials and observed that glass additives enhance the growth in the longitudinal direction of the columnar crystal and had a preferred (0 0 2) orientation. The high $Q \times f$ value of dielectric ceramics is attributed to an increase in composite density when glass is added. Some researchers [14] have also reported that the incorporation of B_2O_3 into the $Ba(Nd_{2-x}Sm_x)Ti_4O_{12}$ crystal changes the lattice constants of the crystal as a result of the diffusion of B atoms to the interstitial sites.

Although the above-mentioned studies have examined the changes that occur when glass and dielectric ceramic are sintered, and noted the effect of secondary phase on the dielectric properties, not much research has been focused on understanding the effect that the ion interdiffusion between alkali-borosilicate glass and $Ba_{0.88}(Nd_{1.40}Bi_{0.42}La_{0.30})Ti_4O_{12}$ ceramic has on the crystal structure and dielectric properties. In this study, an alkali-borosilicate glass of low softening temperature was added to $Ba_{0.88}(Nd_{1.40}Bi_{0.42}La_{0.30})Ti_4O_{12}$ dielectric ceramic to investigate the effect of glass additives on the microstructure and dielectric properties of ceramics. An XRD, EPMA, DSC, and TEM with an attached energy dispersive X-ray spectrometer, were used to perform more accurate analysis to address the above-mentioned questions.

2. Experimental procedures

The materials used in this study were $Ba_{0.88}(Nd_{1.40}Bi_{0.42}La_{0.30})Ti_4O_{12}$ ceramic (abbreviated as B(NBL)T, Prosperity Dielectric, NPO-110) and alkali-borosilicate glass powder (SiO_2–B_2O_3–Al_2O_3–CaO–Na_2O–K_2O–BaO, China Glaze, CS-9609). The average particle sizes of B(NBL)T ceramic and glass powder were 3.2 μm and 4.6 μm, respectively. The physical properties and compositions of these materials are listed in Table 1.

B(NBL)T ceramic and glass powders of various volumetric ratios (50/50, 45/55, and 40/60) were ball-milled in an isopropyl alcohol (IPA) solvent containing zirconia balls 3 mm in diameter for 24 h in a polyethylene bottle. A solution composed of an acrylic resin (Elvacite, 2046) and IPA was then mixed with the milled powder and spray-dried into spherical granules. Granules with a mean particle size of around 70 μm were obtained through sieving and uniaxially pressed into pellets that were 15 mm in diameter and either 4 mm or 8 mm in thickness at a pressure of 90 MPa. Sintering was then carried out in air. The thermal profile included heating at a rate of 2 °C/min to 350 °C, held for 30 min, followed by heating at a rate of 2 °C/min to 500 °C, held for 30 min, and finally heating at a rate of 3 °C/min to a sintering temperature ranging between 750 °C and 950 °C and held for a period ranging from 30 min to 120 min.

The crystal structure of the sintered composites were analyzed using an X-ray diffractometer (XRD, REGAKU, DMAX-VB) at 40 kV and 100 mA, using Cu Kα (λ = 0.15418 nm) radiation. In a scanning range (2θ) of 10°–50°, the scanning rate was 3°/min and the scanning interval was 0.05°. Back-scattered electron images (BEI) of the polished specimens were examined along with electron probe microanalysis (EPMA), using a scanning electron microscope (JEOL, JXA-8900R) operated at an accelerating voltage of 20 kV. The interfacial reaction between B(NBL)T ceramic and glass was examined using EPMA. The specimen used was prepared by firing a piece of green glass compact on top of a densified B(NBL)T substrate at a heating rate of 5 °C/min from room temperature to 950 °C in air.

A transmission electron microscope (AEM, JEOL-2010) with an energy dispersive X-ray spectrometer (EDS, OXFORD, ISIS-300) attached was operated at an accelerating voltage of 200 kV. Selected area diffraction (SAD) patterns were recorded at a camera length of 100 cm and an aperture of 150 nm. The electron beam size of this EDS analysis was 7 nm and the analyzed area was approximately 50 nm in diameter. Quantitative composition analysis of the selected area was carried out using the Cliff-Lorimer Ratio of Thin Section, using copper as the calibration standard. The absorption correction and fluorescence correction were neglected and only the atomic number correction was carried out using the attached software. A TEM analysis of a silicon specimen (Si, $a = 0.5431$ nm, JCPDS 27-1402) was used for calibration from which the SAD pattern of Si [1 1 0] was obtained and the lattice parameter calculated to be 0.552 nm. As this value exceeded the standard value of Si by approximately 1.7%, this instrumentation error (1.7%) was deducted directly from the results of subsequent experiments.

Table 1
Physical properties and compositions of B(NBL)T ceramic powder and alkali-borosilicate glass powder.

Material	Density (g/cm^3)	Mean particle size (μm)	Composition (wt.%)						
B(NBL)T	5.64	3.2	TiO_2	Nd_2O_3	BaO	Bi_2O_3	La_2O_3		
			37.6	28.4	16.2	11.9	5.9		
Glass	2.45	4.6	SiO_2	Al_2O_3	B_2O_3	CaO	K_2O	Na_2O	BaO
			38.1	17.3	16.9	12.1	6.8	4.7	4.1

Glass transition temperatures (T_g) were investigated using a thermal analyzer (SETARAM, SETSYS-TGA, TG/DSC) at a heating rate of 10 °C/min from room temperature to 1100 °C in air. The dielectric properties were measured using an RF impedance analyzer (HP 4291B) set to a frequency of 1 GHz, while the resonant frequencies were measured via a parallel plate dielectric resonator on a network analyzer (AGILENT 8722ES) using Hakki and Coleman's method. The diameter-to-height ratio of specimens was maintained between 1.8 and 2.3.

3. Results and discussion

3.1. X-ray diffraction analysis

The X-ray diffraction patterns of samples sintered under various conditions are shown in Fig. 1(a). Note that the X-ray diffraction patterns of the original B(NBL)T powder and those sintered for 1 h at 1260 °C, 1360 °C, and 1460 °C are almost identical with all exhibiting an orthorhombic crystalline structure. These results are consistent with those reported by Silva et al. [15] for $BaNd_2Ti_4O_{12}$. Fig. 1(b)–(d) shows the X-ray diffraction patterns of B(NBL)T/glass composites with 50 vol.%, 55 vol.%, and 60 vol.% glass additions, respectively, sintered at various temperatures for 2 h. It can been seen that as the sintering temperature increased, the peak intensity of the (3 2 0) plane of B(NBL)T increased, whereas a decrease was observed for the (4 0 1) plane. Such a development could be attributed to a change in the preferred orientation of the B(NBL)T crystals, due to wetting by the glass phase and possibly a phase reaction at the sintering temperature [16]. Similar observations were also reported for aluminosilicate glass addition to BaO–Nd_2O_3–Sm_2O_3–TiO_2, which promoted development of columnar grains of (0 0 2) preferred orientation [17].

In addition to a change in intensity, it can also be observed that as the sintering temperature increased, the diffraction angle of (3 2 0) plane decreased. This indicates that when B(NBL)T is sintered in the presence of the glass phase, not only does a change in preferred orientation but also a change in lattice parameters. The diffraction angles of the (3 2 0), (4 0 1), and (3 0 3) planes of the B(NBL)T/glass 45/55 vol.% composite sintered at 950 °C for 2 h were 32.80°, 31.55°, and 29.05°, respectively. A least square regression of the three equations yielded lattice constants of $a = 1.154$ nm, $b = 0.776$ nm, and $c = 1.536$ nm. Compared with the JCPDS data of $BaNd_2Ti_4O_{12}$ ceramics (No. 35-0331, $a = 1.147$ nm, $b = 0.769$ nm, $c = 1.552$ nm), the lattice constants were larger by 0.6% in the a-axis and 0.9% in the b-axis but smaller by 1.0% in the c-axis.

From previous studies, it was found of the addition of B_2O_3 into a $Ba(Nd_{2-x}Sm_x)Ti_4O_{12}$ crystal would result in changes in the crystal's lattice constants due to the diffusion of B atoms

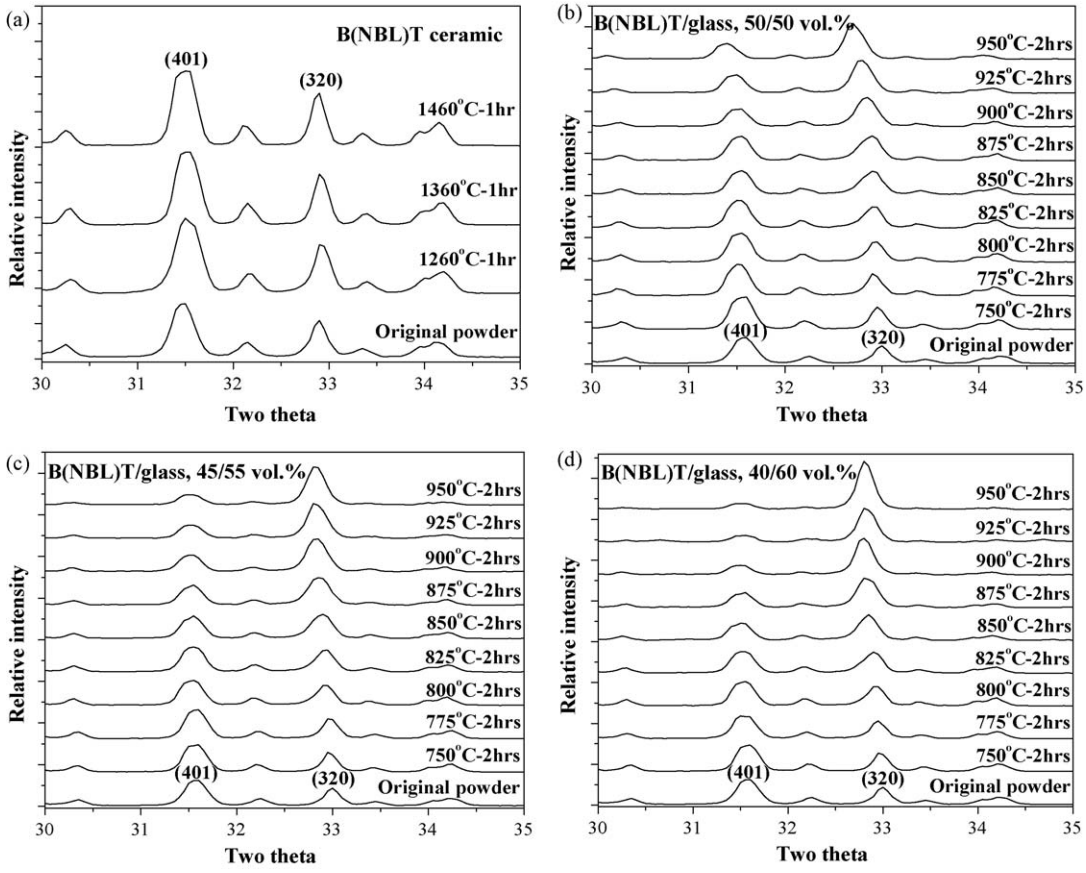

Fig. 1. X-ray diffraction patterns at various sintering temperatures of (a) B(NBL)T ceramic, (b) B(NBL)T/glass 50/50 vol.%, (c) B(NBL)T/glass 45/55 vol.%, (d) B(NBL)T/glass 40/60 vol.%.

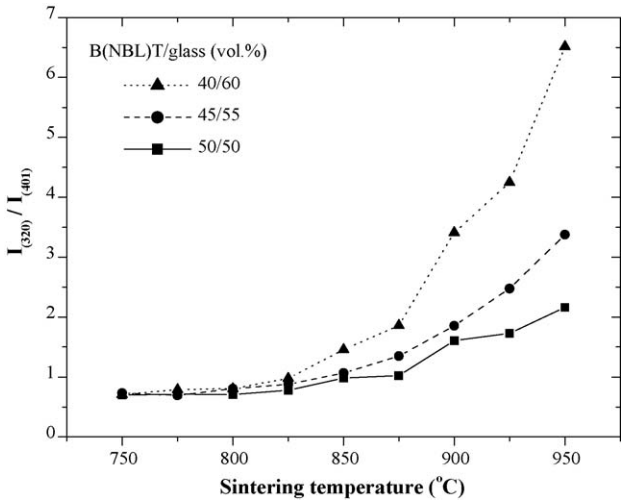

Fig. 2. Intensity ratio $I_{(3\ 2\ 0)}/I_{(4\ 0\ 1)}$ as a function of sintering temperature for B(NBL)T/glass composites with 50 vol.%, 55 vol.%, and 60 vol.% glass sintered for 2 h in air.

into the interstitial sites [14]. Similarly, interaction between the B(NBL)T ceramic and the glass phase could have caused a change in the preferred orientation, as well as a shift in the diffraction angles of the XRD patterns. Fig. 2 shows the relationship between the sintering temperature and ratio of the peak intensity of (3 2 0) to that of (4 0 1), $I_{(3\ 2\ 0)}/I_{(4\ 0\ 1)}$, for B(NBL)T/glass composites with 50 vol.%, 55 vol.%, and 60 vol.% glass additions, respectively. It can be observed that not only an increase in sintering temperature but also an increase in the volume percentage of glass phase significant increase the $I_{(3\ 2\ 0)}/I_{(4\ 0\ 1)}$ ratio.

3.2. EPMA analysis

Fig. 3 shows the BEI photograph and corresponding mappings of Ba, Na, and Ca in a B(NBL)T/glass 45/55 vol.% composite, sintered at 750 °C for 30 min. Based on the color contrasts in the EPMA mappings, it can be seen that the concentration of Ba within the ceramic is higher than that in the glass phase, whereas the concentration of Na and Ca in the glass phase is higher than that within the ceramic. Similar results were also observed in the B(NBL)T/glass 50/50 vol.%, and B(NBL)T/glass 40/60 vol.% composites. The interdiffusion of Ba, Na, and Ca between the B(NBL)T ceramic and the glass phase is not apparent most likely due to a low sintering temperature and insufficient held time.

The BEI photograph and corresponding mappings of Ba, Na, and Ca in a B(NBL)T/glass 45/55 vol.% composite, sintered at 950 °C for 2 h are shown in Fig. 4. It can be observed that the concentration of Ba was reduced slightly around the edge of the ceramic, as a result of dissolution of Ba into the glass phase. Na and Ca, on the other hand, diffused into the ceramic and therefore a slight increase in the concentration of these two elements was found near the edge of the ceramic. Similar results were also observed in the B(NBL)T/glass 50/50 vol.%, and B(NBL)T/glass 40/60 vol.% composites.

Due to the resolution of the sintered composite BEI photograph was insufficient to examine the interface between the B(NBL)T ceramic and the glass phase after sintering, a

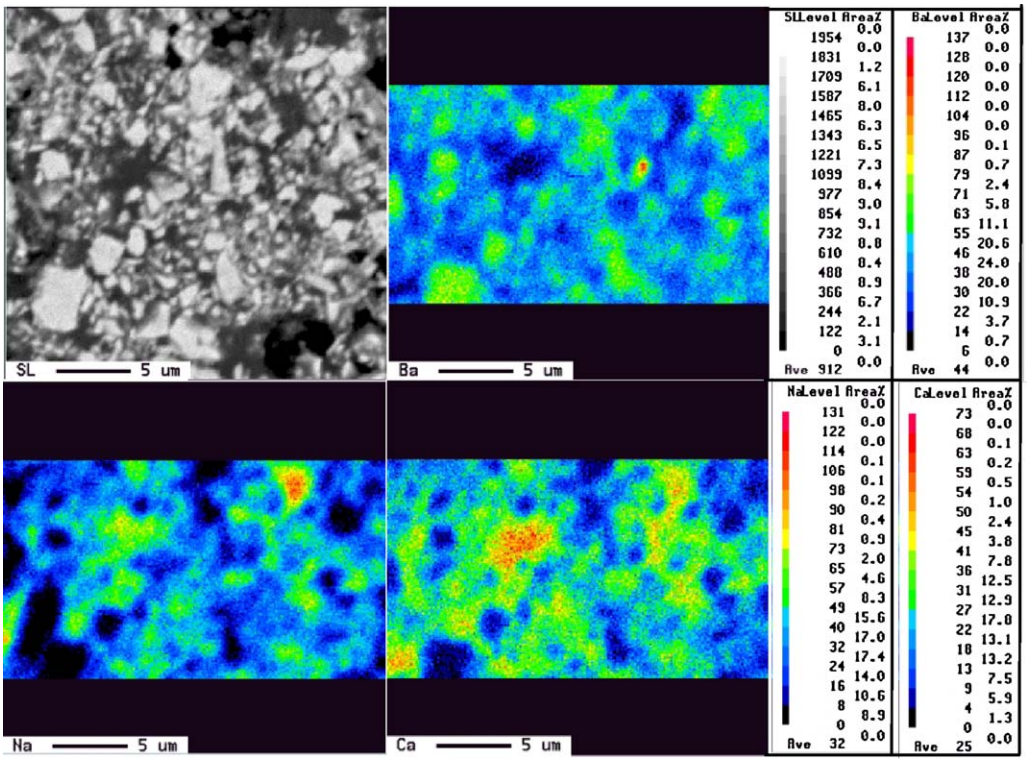

Fig. 3. BEI photograph and EPMA mappings of, Ba, Na, and Ca of a B(NBL)T/glass 45/55 vol.% composite, sintered at 750 °C for 30 min. The B(NBL)T ceramics (bright domain), and the glass phase (dark domain).

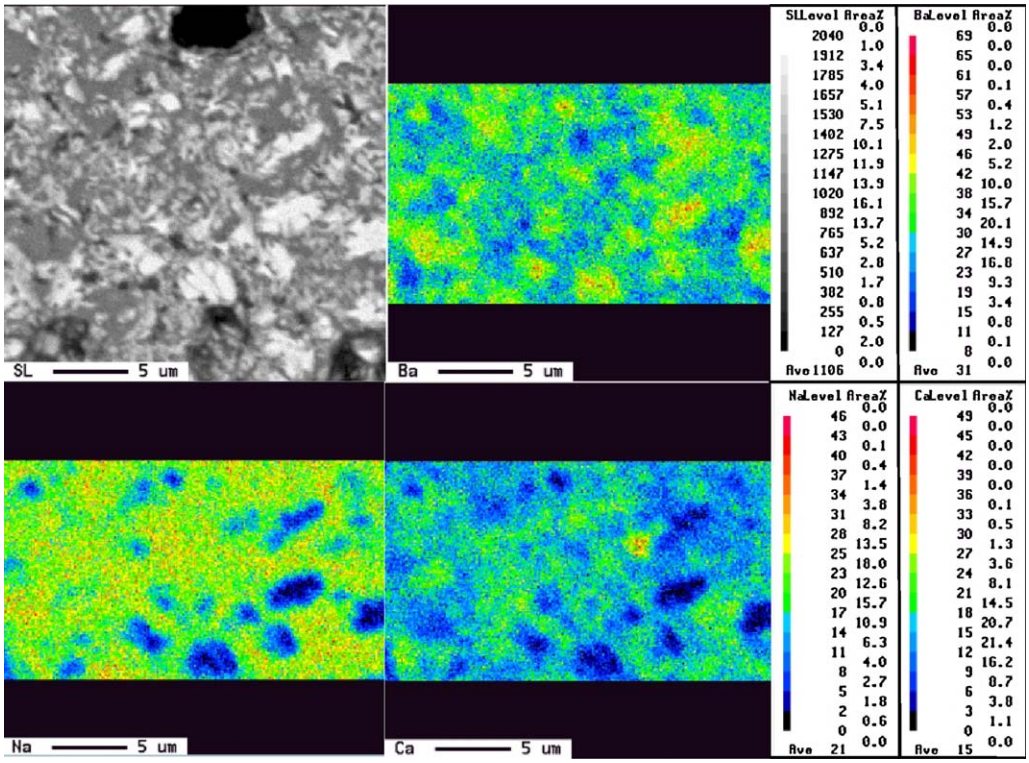

Fig. 4. BEI photograph and EPMA mappings of Ba, Na, and Ca in a B(NBL)T/glass 45/55 vol.% composite, sintered at 950 °C for 2 h. The B(NBL)T ceramics (bright domain), and the glass phase (gray domain).

reaction couple was designed. Fig. 5 shows the BEI photograph of a B(NBL)T/glass reaction couple, sintered at 950 °C for 2 h. Based on the BEI photograph it is evident that an interface of approximately 2 μm in thickness exists between the two original phases. Previous research have reported interdiffusion coefficients between Ba^{2+} and Na^{+}, and Ba^{2+} and K^{+} to be approximately 10^{-8} cm^2/s at 950 °C [18]. Based on this finding to apply Fick's second law, the interdiffusion distance after 2 h is estimated to be 100 μm. Therefore, the interfacial reaction might have controlled the growth of this interfacial reaction zone.

The BEI image and corresponding element mappings of Ba, Nd, Bi, La, Ti, Al, Na, Ca, and K in the B(NBL)T/glass interface are shown in Fig. 6. It can be observed that the concentrations of Ba and Bi decreased along the edges of the B(NBL)T ceramic, whereas the opposite trend was observed for Na, Ca, and K. However, Nd, La, Ti, Al, and Si did not show significant changes.

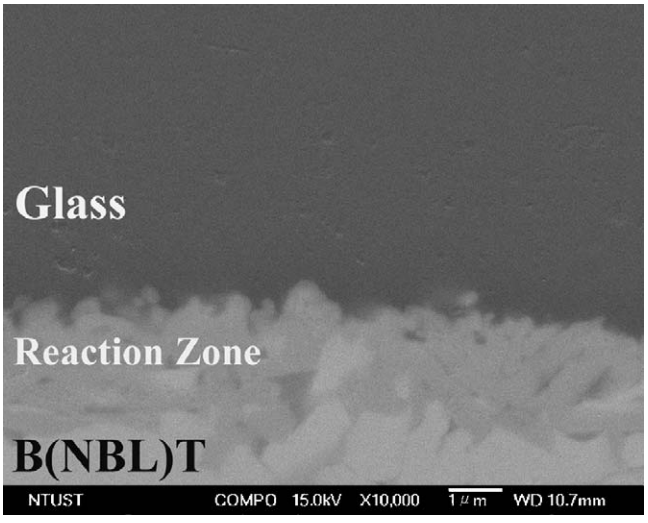

Fig. 5. A BEI photograph of a reaction couple for B(NBL)T and glass, sintered at 950 °C for 2 h.

3.3. TEM analysis

Due to the inadequate resolution of EPMA mappings in the interfacial area, a TEM was used to examine the interface between the B(NBL)T and the glass, and an EDS was performed to measure the composition variation between the ceramic and the glass phase. Fig. 7(a) displays the TEM bright field image of the B(NBL)T/glass 45/55 vol.% composite sintered at 800 °C for 2 h. Fig. 7(b)–(d) shows results from EDS analysis. Taking the average of 4 points along the edge of the B(NBL)T ceramic, the composition at the edge of the B(NBL)T ceramic was estimated to be Ba (7.1 at.%), Nd (8.3 at.%), Bi (1.7 at.%), La (2.6 at.%), Ti (21.3 at.%), Al (0.3 at.%), Na (2.5 at.%), Ca (0.2 at.%), and Si (1.3 at.%). By taking the average of three different points along the edge of the glass, the average composition along the edge of the glass was determined to be Ba (0.5 at.%), Nd (0.2 at.%), Bi (0.1 at.%), La (0.2 at.%), Ti (0.7 at.%), Al (6.4 at.%), Na (0.6 at.%), Ca (0.2 at.%), and Si (29.5 at.%).

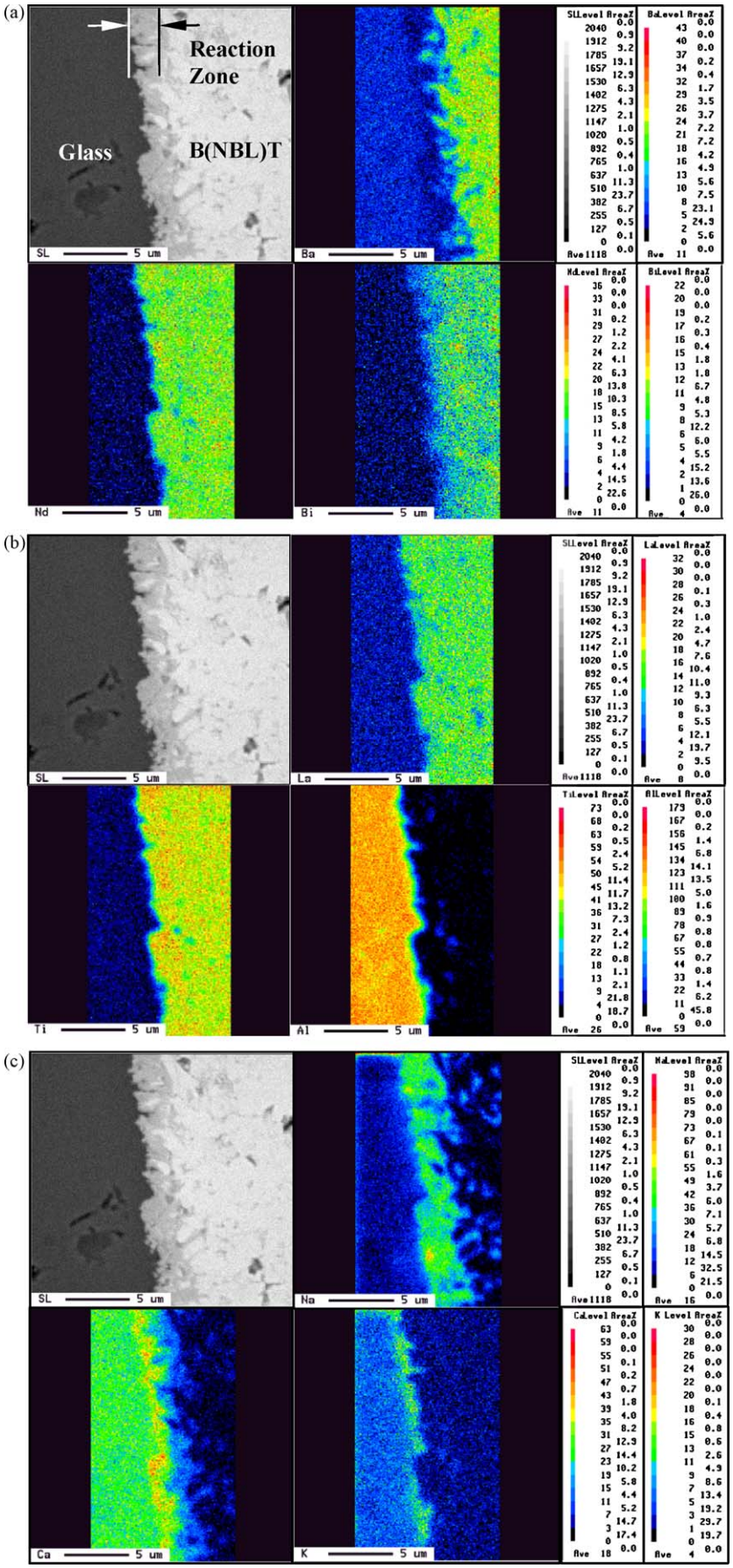

Fig. 6. BEI photographs and EPMA mappings of (a) Ba, Nd, Bi, (b) La, Ti, Al, (c) Na, Ca, K of a B(NBL)T and glass reaction couple, sintered at 950 °C for 2 h.

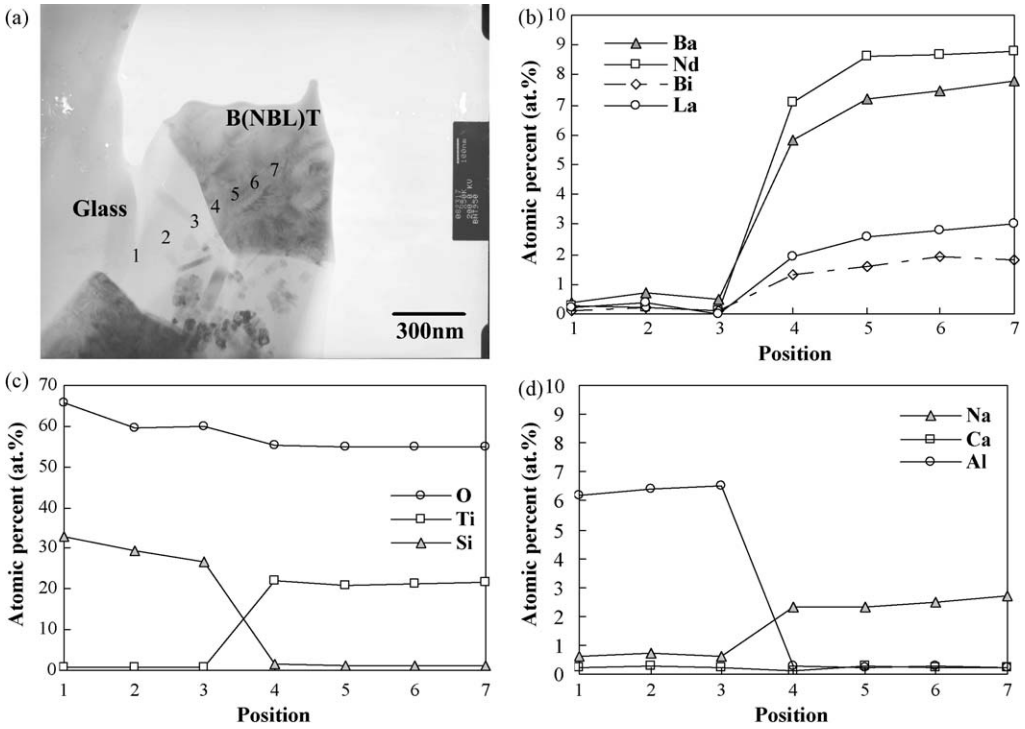

Fig. 7. B(NBL)T/glass 45/55 vol.% composite sintered at 800 °C for 2 h: (a) TEM bright field image, (b)–(d) EDS composition analysis.

Fig. 8(a) displays the TEM bright field image of a B(NBL)T/glass 45/55 vol.% composite sintered at 950 °C for 2 h. It can be seen that the B(NBL)T phase is rectangular in shape, implying that interfacial reaction might have influenced the growth of the B(NBL)T crystal, which is consistent with conclusions drawn from previous research [16]. Fig. 8(b)–(d) shows the EDS analysis results of the B(NBL)T/glass composite. The average concentration along the edge of the B(NBL)T ceramic for Ba, Nd, Bi, and Ti were 2.8 at.%, 7.3 at.%, 0.4 at.%, and 18.0 at.%, respectively; both were lower than that of the specimen sintered at 800 °C (4.3 at.%, 1.0 at.%, 1.3 at.%, and 3.3 at.%, respectively). La (2.2 at.%), and Al

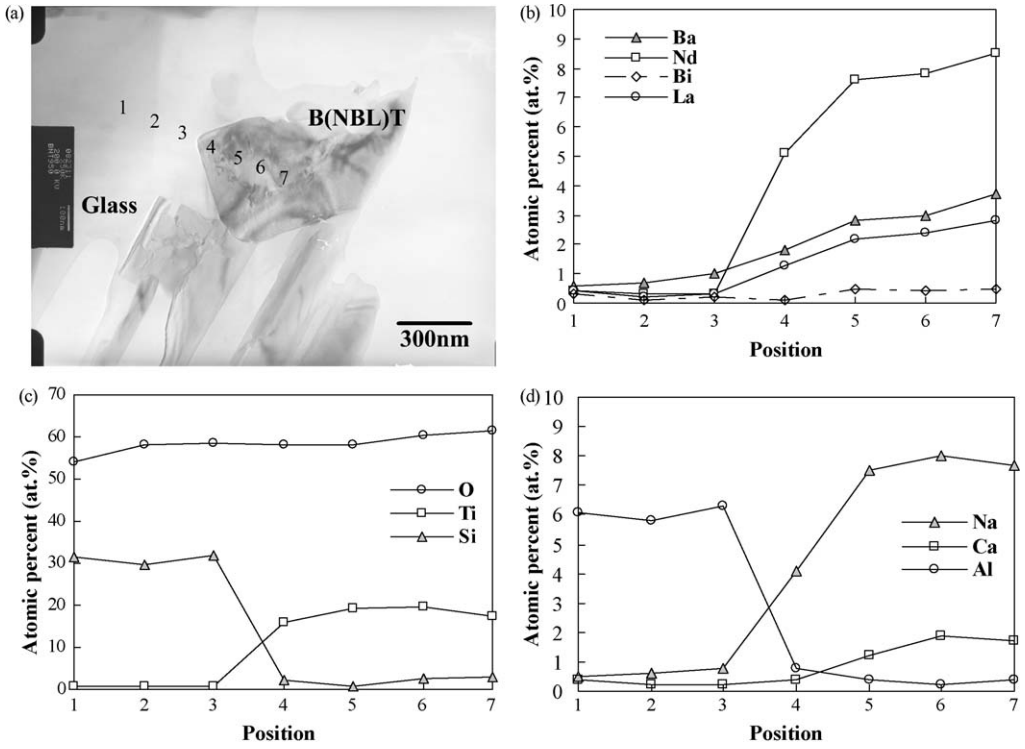

Fig. 8. B(NBL)T/glass 45/55 vol.% composite sintered at 950 °C for 2 h: (a) TEM bright field image, (b)–(d) EDS composition analysis.

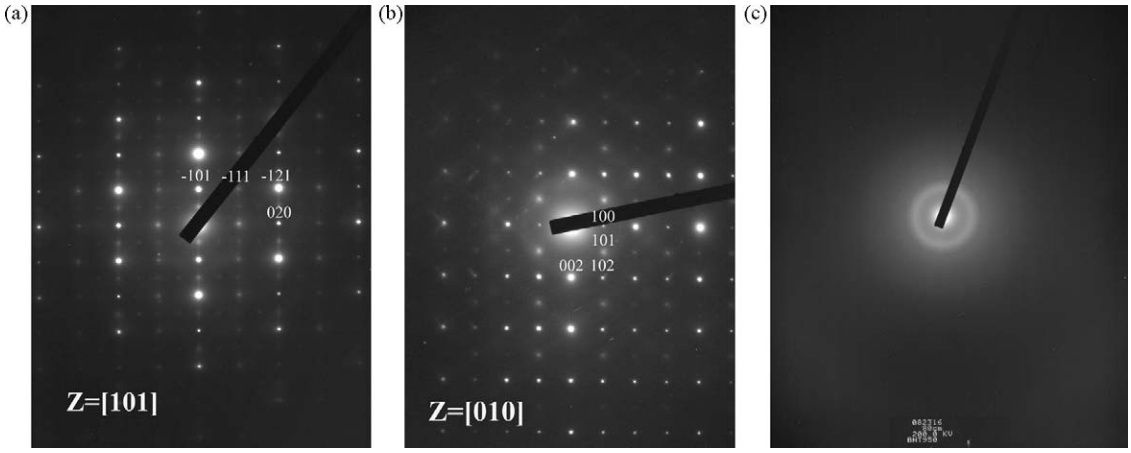

Fig. 9. SAD pattern of a B(NBL)T/glass 45/55 vol.% composite sintered at 950 °C for 2 h, B(NBL)T phase zone axis: (a) [1 0 1], (b) [0 1 0], and (c) SAD pattern of glass.

(0.4 at.%) did not show significant differences as compared with that of the specimen sintered at 800 °C. The average concentrations of Na (6.8 at.%), Ca (1.3 at.%), and Si (2.1 at.%) were higher than that of the specimen sintered at 800 °C (4.3 at.%, 1.1 at.% and 0.8 at.%, respectively).

The average concentrations of Ba (0.8 at.%), Nd (0.3 at.%), Bi (0.2 at.%), and La (0.3 at.%) near the edge of glass were higher than that of the 800 °C specimen (0.3 at.%, 0.1 at.%, 0.1 at.%, and 0.1 at.%, respectively). For Ti (0.7 at.%), Al (6.1 at.%), Na (0.6 at.%), Ca (0.3 at.%), and Si (30.8 at.%), no significant changes occurred. It is evident that during sintering an ionic exchange took place with the glass phase wetting the B(NBL)T, resulting in a change of the preferred crystal plane from (4 0 1) to (3 2 0) and the variation in lattice parameters as shown through XRD analysis. The relationships that exist between the composition, microstructure, and dielectric properties of a B(NBL)T/glass composite will be discussed in the next section.

Fig. 9 (a) and (b) shows the select area diffraction (SAD) patterns of the B(NBL)T phase along the zone axis of [1 0 1] and [0 1 0]. From the diffraction patterns, it can been seen that the B(NBL)T phase had an orthorhombic crystalline structure with lattice parameters of $a = 1.156$ nm, $b = 0.772$ nm, and $c = 1.543$ nm. Compared with the JCPDS data of the $BaNd_2Ti_4O_{12}$ ceramic, the lattice parameters of the B(NBL)T phase were larger by 0.8% in the *a*-axis and 0.4% in the *b*-axis but smaller by 0.6% in the *c*-axis. The small difference in the lattice parameters between the two ceramics is likely caused by the interdiffusion of Ba^{2+}, Bi^{3-} ions of the B(NBL)T ceramic with the Na^+, Ca^{2+} and K^+ ions of glass. However, as the crystal structure of B(NBL)T phase is extremely complex, it is difficult to determine the affect of ion exchanges on lattice parameters using the rule of mixtures. On the other hand, Fig. 9(c) shows the SAD pattern of the glass, which reveals an amorphous structure.

3.4. Dielectric properties

Fig. 10 shows the differential scanning calorimetry (DSC) patterns of the glass powder, a B(NBL)T/glass 40/60 vol.% composite, and a B(NBL)T/glass 50/50 vol.% composite. The transition temperature of the glass phase (T_g) showed two discrete temperatures, 548 °C (T_{g_1}) and 656 °C (T_{g_2}): a result possibly caused by the phase separation of glass during heating. When the sintering temperature increases above the glass

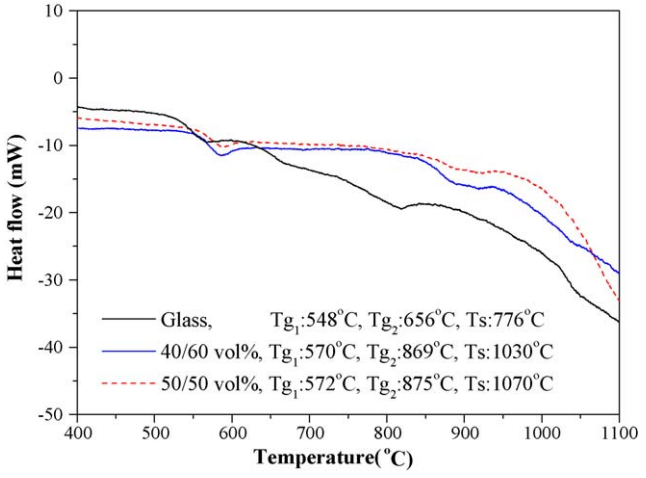

Fig. 10. DSC patterns of the glass powder, the B(NBL)T/glass 40/60 vol.% composite, and the B(NBL)T/glass 50/50 vol.% composite.

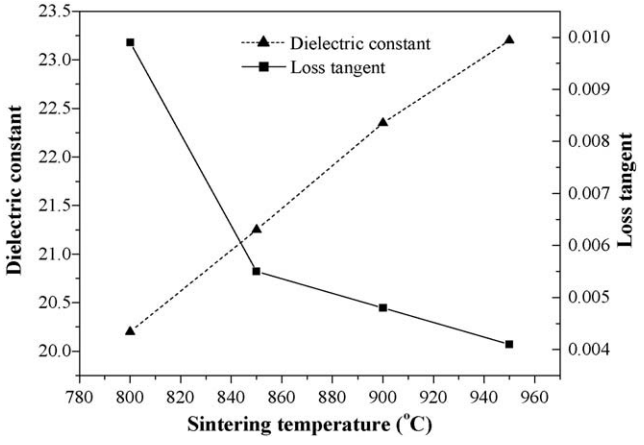

Fig. 11. Dielectric properties as a function of sintering temperature for a B(NBL)T/glass 45/55 vol.% composite, sintered in air for 2 h.

Table 2
Sintered density and dielectric properties of glass, B(NBL)T, and B(NBL)T/glass composites under various sintering conditions.

Specimens	ρ (g/cm^3)	ε_r	tan δ	f (GHz)	$Q \times f$ (GHz)
Glass at 700 °C (at 1 GHz)	2.45	6.8[a]	2×10^{-3}[a]	–[a]	–[a]
B(NBL)T at 1260 °C	5.51	90.32	1.3×10^{-3}	3.46	2586
B(NBL)T at 1360 °C	5.61	94.30	1.2×10^{-3}	3.42	2855
B(NBL)T at 1460 °C	5.40	88.42	1.9×10^{-3}	3.50	1878
B(NBL)T/glass 50/50 vol.% at 950 °C	2.98	20.5	4.9×10^{-3}	6.67	1354
B(NBL)T/glass 45/55 vol.% at 950 °C	3.36	23.2	4.1×10^{-3}	6.67	1620
B(NBL)T/glass 40/60 vol.% at 950 °C	3.34	20.3	5.2×10^{-3}	7.11	1372

[a] The dielectric constant (ε_r) and loss tangent (tan δ) are measured at a test frequency of 1 GHz, as the resonance frequency of glass is higher than the limit of the test equipment, which is 12 GHz (Q = 1/tan δ).

transition temperature, thermal activation occurs and the glass phase is softened. For the glass powder, the commencing softening temperature (T_s) was 776 °C. For the B(NBL)T/glass 40/60 vol.% composite, the glass transition temperatures T_{g_1} and T_{g_2} were around 570 °C and 869 °C and the commencing softening temperature was 1030 °C. For the B(NBL)T/glass 50/50 vol.% composite, both the two discrete glass transition temperatures and the softening temperature increased. The glass transition temperatures increased to about 572 °C (T_{g_1}) and 875 °C (T_{g_2}), and the commencing softening temperature increased to 1070 °C. Such increases in glass transition temperatures (T_g) and softening temperature (T_s) were not completely attributed by the volume percentage of glass. It is believed that the exchange of Na^+, Ca^{2+}, and K^+ ions with Ba^{2+} and Bi^{3-} ions caused the dissolution of larger Ba^{2+} and Bi^{3-} ions into the glass phase and the loss of smaller Na^+, Ca^{2+}, and K^+ ions from the glass phase, resulting in increases in glass transition temperatures and softening temperatures.

Fig. 11 shows the relationship between the dielectric properties and the sintering temperature for the B(NBL)T/glass 45/55 vol.% composite, sintered in air for 2 h. As the sintering temperature increased, the dielectric constant increased, but the loss tangent decreased. Normally, an increase in the sintered density results only in an increase of the dielectric constant and not in a decrease of the dielectric loss. Thus, a decrease in the dielectric loss with an increase in the sintering temperature must have been caused by the phase reaction between the B(NBL)T ceramic and the glass phase, resulting in an ionic exchange between Na^+, Ca^{2+}, K^+ ions and Ba^{2+}, Bi^{3-} ions in the composite. This would cause a decrease in the electrical resistivity of the glass phase, which in turn would yield a decrease in dielectric loss [19]. Similar observations were reported elsewhere, where an increase in the concentration of sodium and potassium ions always resulted in an increase of the loss tangent for many low temperature co-firable dielectric and glass composites [20].

Table 2 shows the sintered densities and dielectric properties of glass, B(NBL)T ceramic, and B(NBL)T/glass composites, processed under various conditions. The B(NBL)T/glass composite with 55 vol.% glass addition had the optimal set of dielectric properties. The lower dielectric constant of the B(NBL)T/glass composite with 50 vol.% glass addition as compared to the one with 55 vol.% is attributed to a lower glass content, which translates to a lower sintered density. On the other hand, the existence of an excessive amount of the glass phase with a lower dielectric constant but a larger dielectric loss than those of the B(NBL)T ceramic, was responsible for the lower dielectric constant and higher dielectric loss of the B(NBL)T/glass composite with 60 vol.% glass addition.

The B(NBL)T/glass composites do not achieve dielectric constant values estimated from the rule of mixtures, but rather exhibits higher dielectric losses, which arise from the motion of the alkali ions (Na^+ and K^+) in the glass phase [21]. The substantial deviation of the measured dielectric constant from that estimated by the rule of mixtures is a percolation phenomenon and is believed to arise from the high threshold volume percentage of the B(NBL)T phase that is required to induce a dielectric response in the composite structure [22]. Consequently, in order to further increase the dielectric constant of the composites, a higher volume percentage of B(NBL)T and a better sintering aid are required.

4. Conclusions

From the XRD pattern, it can be seen that the peak intensity ratio $I_{(3\,2\,0)}/I_{(4\,0\,1)}$ of B(NBL)T not only increased with an increase in sintering temperature, but also with an increase in the volume percentage of the glass phase. This is attributed to interactions between the B(NBL)T ceramic and the glass phase, which caused a change in the preferred orientation, as well as lattice parameters, of the crystal. EPMA mapping and TEM analysis reveal that the concentrations of Ba and Bi decreased along the edge of the B(NBL)T ceramic close to the glass phase, while the opposite trend can be seen for Na, Ca, and K. This is evidence that an ionic exchange took place during sintering with the glass phase wetting the B(NBL)T ceramic, resulting in the change in the crystal plane from (4 0 1) to (3 2 0), the change in lattice parameters, the decrease in dielectric loss, as well as the increase in glass transition and softening temperatures. A relatively low sintered density in addition to an excessive amount of the glass phase was responsible for the low dielectric constants of B(NBL)T/glass composites. When sintered at 950 °C for 2 h, the composite with 55 vol.% glass yielded the highest dielectric constant (ε_r = 23.2), the lowest dielectric loss (loss tangent = 4.1×10^{-3}), and a high $Q \times f$ value (1620 GHz, Q = 1/tan δ, f = 6.67 GHz).

References

[1] Y.C. Zhang, Z.X. Yue, Z.L. Gui, L.T. Li, Effects of CaF_2 addition on the microstructure and microwave dielectric properties of $ZnNb_2O_6$ ceramics, Ceram. Int. 29 (2003) 555–559.

[2] C.S. Chen, C.C. Chou, C.S. Chen, I.N. Lin, Microwave dielectric properties of glass-MCT low temperature co-firable ceramics, J. Eur. Ceram. Soc. 24 (2004) 1795–1798.
[3] W.C. Tzou, S.L. Chang, C.F. Yang, Y.C. Chen, Sintering and dielectric properties of $0.88Al_2O_3$–$0.12TiO_2$ microwave ceramics by glass addition, Mater. Res. Bull. 38 (2003) 981–989.
[4] C.C. Cheng, T.E. Hsieh, I.N. Lin, Effects of composition on low temperature sinterable Ba–Nd–Sm–Ti–O microwave dielectric materials, J. Eur. Ceram. Soc. 24 (2004) 1787–1790.
[5] I.S. Cho, D.W. Kim, J.R. Kim, K.S. Hong, Low-temperature sintering and microwave dielectric properties of $BaO(Nd_{1-x}Bi_x)_2O_34TiO_2$ by the glass additions, Ceram. Int. 30 (2004) 1181–1185.
[6] C.L. Huang, M.H. Weng, C.T. Lion, C.C. Wu, Low temperature sintering and microwave dielectric properties of $Ba_2Ti_9O_{20}$ ceramics using glass additions, Mater. Res. Bull. 35 (2000) 2445–2456.
[7] J.H. Jean, T.K. Gupta, Design of low dielectric glass + ceramics for multilayer ceramic substrate, IEEE Trans. Compon. Pack. Manuf. Technol. B: Adv. Pack. 17 (1994) 228–233.
[8] O. Dernovsek, A. Naeini, G. Preu, W. Wersing, M. Eberstein, W.A. Schiller, LTCC glass–ceramic composites for microwave application, J. Eur. Ceram. Soc. 21 (2001) 1693–1697.
[9] B.H. Jung, S.J. Hwang, H.S. Kim, Glass–ceramic for low temperature co-fired dielectric ceramic materials based on La_2O_3–B_2O_3–TiO_2 glass with BNT ceramics, J. Eur. Ceram. Soc. 25 (2005) 3187–3193.
[10] P.V. Bijumon, M.T. Sebastian, Influence of glass additives on the microwave dielectric properties of $Ca_5Nb_2TiO_{12}$ ceramics, Mater. Sci. Eng. B 123 (2005) 31–40.
[11] Y.W. Liu, P. Lin, Effects of glass additions on microstructure and microwave dielectric properties of $La_4Ti_9O_{24}$ ceramics, Mater. Chem. Phys. 92 (2005) 98–103.
[12] J.A. Lee, J.H. Lee, J.J. Kim, Effect of borate glass additives on the sintering behaviour and dielectric properties of $BaTi_4O_9$ ceramics, J. Eur. Ceram. Soc. 26 (2006) 2135–2138.
[13] L.C. Chang, B.S. Chiou, W.H. Lee, Effect of glass additions on the sintering behaviors and electrical microwave properties of BaO–Nd_2O_3–Sm_2O_3–TiO_2 ceramics, J. Mater. Sci. Mater. Electron. 15 (3) (2004) 153–158.
[14] L.C. Chang, B.S. Chiou, Effect of B_2O_3 nano-coating on the sintering behaviors and electrical microwave properties of $Ba(Nd_{2-x}Sm_x)Ti_4O_{12}$ ceramics, J. Electroceram. 13 (1–3) (2004) 829–837.
[15] A. Silva, F. Azough, R. Freer, C. Leach, Microwave dielectric ceramics in the system BaO–Li_2O–Nd_2O_3–TiO_2, J. Eur. Ceram. Soc. 20 (2000) 2727–2734.
[16] C.L. Liao, K.H. Lin, S.T. Lin, Effects of alkali-borosilicate glass additions on the microstructure and dielectric properties of $Ba_{0.88}(Nd_{1.40}Bi_{0.42}$-$La_{0.30})Ti_4O_{12}$, J. Ceram. Process. Res. 9 (6) (2008) 562–568.
[17] L.C. Chang, B.S. Chiou, Electrical behavior of BaO–Nd_2O_3–Sm_2O_3–TiO_2 with glass/oxide additives analyzed by impedance spectroscopy, J. Electroceram. 15 (1) (2005) 75–81.
[18] V.S. Grigor'ev, A.K. Yakhkind, V.Ya. Alaev, Kinetics of the ion-exchange interaction in glass melts containing barium and alkali metal oxides, Sov. J. Glass Phys. Chem. 14 (2) (1989) 126–131.
[19] W.D. Kingery, H.K. Bowen, D.R. Uhlmann, Introduction to Ceramics, 2nd ed., John Wiley & Sons, Inc., 1976, pp. 879–945.
[20] G. Kniajer, K. Dechant, P. Apte, Low loss, low temperature cofired ceramics with higher dielectric constants for multichip modules (MCM), in: Proc. SPIE Int. Soc. Opt. Eng., 1997, 121–127.
[21] C. Siligardi, C. Leonelli, Y. Fang, D. Agrawal, Modifications on bulk crystallization of glasses belonging to M_2O–CaO–SiO_2–ZrO_2 system in a 2.45 GHz microwave field, Mater. Res. Soc. Symp. Proc. 430 (1996) 429–434.
[22] C. Huang, Q. Zhang, Enhanced dielectric and electromechanical responses in high dielectric constant all-polymer percolative composites, Adv. Funct. Mater. 14 (5) (2004) 501–506.